





Digital Retinal Fundus Imaging: An AI-Assisted Effective Machine Learning Model for Detecting Ocular Pathology

Muhammad Adee Asghar, Sobia Shafiq, Jawwad Ibrahim, Malaika Saeed

Department of Computer Science, National University of Modern Languages, Khadim Hussain Road, Rawalpindi

*Correspondence; Muhammad Adeel Asghar, adeel.asghar@numl.edu.pk

Citation | Asghar. M. A, Shafiq. S, Ibrahim. J, Saeed. M, "Digital Retinal Fundus Imaging: An AI-Assisted Effective Machine Learning Model for Detecting Ocular Pathology", IJIST, Vol. 07 Issue. 02 pp 881-896, May 2025

DOI https://doi.org/10.33411/ijist/202572881896

Received | April 17, 2025, Revised | May 12, 2025, Accepted | May 15, 2025, Published | May 16, 2025.

cular pathology is the study of employing digital fundus imaging to diagnose various eye-related diseases. Macular degeneration, cataracts, glaucoma, and diabetic retinopathy are among these eye diseases. To distinguish between these illnesses, a manual examination of the human eye is performed. Since the work is arduous, we have used many complex machine learning techniques in this paper to automatically identify eye disorders using digital retinal fundus imaging. In our initial stage, the dataset is de-noised to avoid misclassification. Additionally, we use Contrasted Limited Adaptive Histogram Equalization (CLAHE) to enhance the images. By adjusting the histograms' adaptive equalization parameters, it is possible to improve the fundus image on each of the RGB channels separately. With the help of three distinct deep CNN models; AlexNet, GoogLeNet, and ResNet50, high-quality features were extracted in the second phase. After merging the features, a composite feature vector was created. This is done to choose characteristics of superior quality. The Bag of Deep Features (BoDF) was used to choose features of the highest caliber. BoDF will assist in lowering the size of the feature so that it can be recognized quickly. Using Mutual Information (MI), comparable features were also eliminated. Support Vector Machine (SVM) and Decision Tree (DT) were then used to classify the model's output to identify ocular diseases. The STARE dataset is used in this research. When compared to current state-of-the-art models, the proposed model is more appropriate and provides an overall classification performance of 94.8% in almost 3 seconds.

Keywords: Ocular Pathology; Retinal Fundus Imaging; Deep Learning; Bag of Deep Features; Mutual Information.

















ResearchGate















Introduction:

Ocular pathology is the branch of study focused on diseases and disorders that affect the eyes. The eye is a highly complex organ that functions by capturing optical signals and converting them into electrical signals, enabling the brain to form a clear visual image. Ocular pathology is a field of study that concentrates on disorders that affect the eyes. To provide the brain with a clear picture, the eye is an extremely complicated system that uses optical signals and converts them into electrical signals [1][2]. Complications involving the eye often have a strong potential to cause irreversible vision loss. These conditions include cataracts, glaucoma, diabetic retinopathy, and age-related macular degeneration [3]. All these disorders require manual examination of the eyes, which is time-consuming. Different machine learning methods have been suggested to quickly identify eye diseases in order to save time. In recent years, numerous machine learning models have been developed, with deep learning emerging as a powerful approach to address these types of problems effectively. Convolution neural networks (CNN), a particular type of neural network, are used frequently for visual image analysis in deep learning [4].

The inaugural World Report on Vision published by the World Health Organization in 2019 [5] estimates that 2.2 billion people worldwide have vision impairment or blindness. Screening diabetic patients for diabetic retinopathy can reduce their risk of blindness by up to 50%. Color fundus camera imaging is a crucial and simple method for identifying several eye conditions, including diabetic retinopathy (DR). Early detection of diabetic retinopathy enables the use of laser therapy to prevent or slow down vision loss and can also encourage patients to manage their diabetes more effectively [6]. The current procedures for detecting and evaluating diabetic retinopathy are labor-intensive, expensive, and dependent upon qualified ophthalmologists [7][8][9][10]. Therefore, detecting and treating diabetic retinopathy automatically at an early stage helps prevent blindness. AMD and Glaucoma can also be detected at an early stage to avoid color blindness and vision loss.

Ocular Pathology and Retinal Fundus:

Ocular pathology is the study of diseases affecting the eye and its surrounding structures, focusing on their causes, effects, and treatment. It also explores how these diseases impact the tissues and functions of the eye [11]. Retinal fundus imaging is one of the medical technologies that has advanced recently. The evolution of medical diagnostic technologies has led to the widespread usage of image processing systems in clinical standard practices. It is a procedure in which a fundus camera captures a picture of the retina [12]. A retina or fundus camera aids a doctor in obtaining a clear image of the retina's inside. Retinal arterioles and venules, which flow through the retina's nerve fiber layer and are the sole section of the retina, are transparent in a typical fundus picture. The typical fundus image used for ocular pathology is shown in Figure 1. The doctors can personally examine the ailment with the help of imaging. These picture collections are used in this article to enhance the classification performance and the accurate detection of ocular diseases.

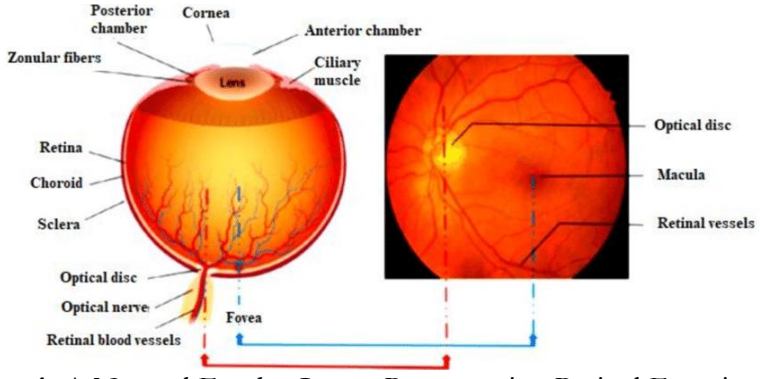


Figure 1. A Normal Fundus Image Representing Retinal Functions [12]



Objectives:

- The dataset was initially denoised during setup. Machine learning algorithms were fed enhanced images. Contrasted Limited Adaptive Histogram Equalization uses this adaptive enhancement (CLAHE). THE CLAHE is useful for fine-tuning the image utilizing the individual Red, Green, and Blue (RGB) channels.
- Three separate machine learning models were used to extract features, GoogLeNet, and ResNet-50, which were then combined to create a set of high-quality features.
- A Mutual Information (MI) approach was devised to minimize the feature dimension. This approach chooses the feature values with the same data and ignores the rest. To verify the relationship information, the probability of each feature value was calculated.
- A feature set was further condensed using the Bag of Deep Data (BoDF) model, which only keeps the high-quality features that are useful for diagnosing the disease while discarding the rest. This will increase performance by 4% while decreasing the feature dimension by up to 63%. This model significantly reduces the model's test and train times for unsupervised learning.
- The model was subsequently evaluated in the last step using the Support Vector Machine (SVM) and Decision Tree techniques.

Related Work:

The traditional diagnosis of glaucoma by manual inspection of fundus imaging requires highly certified and skilled individuals, and it is heavily reliant on their subjective assessments [13]. The detection of eye-related diseases is critical in order to protect humans from blindness. Many treatments have been conducted; however early detection is extremely difficult. Nevertheless, in medical imaging (for example, retinal fundus pictures), early-stage identification of lesions and anomalies remains a challenge. Many researchers have researched eye disorders such as diabetes and glaucoma. Diabetic eye disease (DED) is a group of vision problems that affect diabetics. The authors of [14] use a Convolutional Neural Network to detect DED (CNN). To enhance performance, they combined handcrafted features with neural network features. They also examined how traditional image pre-processing can improve the accuracy of early-stage Dry Eye Disease (DED) detection using deep learning models. With this approach, the model achieved an accuracy of 91.43%. Similarly, [15] and [16] construct a CNN model to classify Glaucoma severity. Glaucoma is a series of visual disorders that cause nerve damage. Early detection of glaucoma is advantageous for improved eyesight. Both authors used retinal fundus imaging to detect the illness and the CLAHE process to improve the images. Texture-based characteristics such as the Zernike moment, chip histogram, and harelike features have been computed from high-frequency modes. The classification accuracy achieved is 89.45% and 94% respectively when classified using the Support Vector machine classifier.

The author in [17] uses a neural network approach to identify Glaucoma illness. A total of 163 glaucoma-affected eyes, classified into four types of optic discs by three glaucoma specialists, were randomly split into training and test datasets. The accuracy achieved with the 10-fold cross-validation and Support Vector Machine (SVM), Nave Bayes (NB), and Decision Tree (DT) is 87.1%, 85.2%, and 90.2%, respectively. These quantifiable factors enabled the trained NN to categorize glaucomatous optic discs with rather high accuracy without the need for color fundus images. The author in [18] detects Glaucoma illness using GoogLeNet, EfficientNet, MobileNet, and DenseNet. In this procedure, retinal fundus imaging is performed to attain an average accuracy of 83.4%.

With advances in image sensors and smartphone technologies, it is now possible to capture high-definition photographs without the need for expensive camera equipment. The Fundus Imaging technology is being used in research to automatically detect eye problems.



Numerous researchers are actively working on developing the Internet of Medical Things (IoMT) [19], [20], and [21]. Local Binary Pattern (LBP) and Local Energy-based Shape Histogram (LESH) are used to detect diabetic illness (LESH). The model is then categorized using SVM, which achieves 93.1% accuracy. [20] and [21] employ transfer learning methodology to combine features from various machine learning models. The authors of [20] and [21] successfully improved classification performance using the DenseNet and U-Net models. The authors in [22] proposed a Long Short-Term Memory (LSTM) model for detecting diabetic retinopathy and age-related macular degeneration. Using this approach, they achieved a sensitivity of 94.95% and a specificity of 98.31%. Similarly, [23][24] used monoscopic fundus images rather than colored fundus images.

Machine learning techniques have been widely applied in the classification of various diseases in the medical industry over the last two decades. Deep learning uses neural networks to learn underlying features in data. It is frequently more concerned with data representation than with task-specific algorithms. In [25], a variety of machine learning techniques such as Decision Trees (DT), Logistic Regressions (LR), Discriminant Analysis (DA), Support Vector Machines (SVM), k-nearest Neighbors (k-NN), and ensemble learners are employed. SVM achieves an average classification accuracy of 77.8%. The developers of [26] proposed a machine-learning model for detecting three ocular diseases: diabetic retinopathy (DR), agerelated macular degeneration (AMD), and glaucoma.

The author in [27], employs retinal fundus imaging to diagnose three eye disorders using 8739 retinal fundus pictures. In their work, they employed the Messidor-2 dataset and a multiple upgraded Inception-v4 assembling approach to detect eye disorders. The model with this scheme achieved 95% accuracy and 98.5% respectively [28][29][30][31][32][33]. Methodology:

Experimental Design:

The proposed scheme combines high-quality feature selection with the implementation of a Bag of Deep Features (BoDF) to detect ocular disease using a multimodal scheme. The dataset images were first enhanced using the CLAHE enhancement algorithm, after which features from three different neural networks were extracted and combined to form a complete feature vector. Mutual Information is used to discard all similar features and then use the full BoDF approach to select high-quality features. This approach improves overall classification performance by lowering the computational cost of the multi-model approach. The proposed approach begins with denoising as the first step, followed by image augmentation. Subsequently, features are extracted using a multimodal neural network. The focus of this study is featuring defusing, which entails combining features from all models to generate a combined feature vector. This will aid in the selection of high-quality features. BoDF was employed to reduce the high-dimensional feature set, enabling efficient classification performance within a shorter processing time. The suggested work steps are outlined one by one in the following sections.

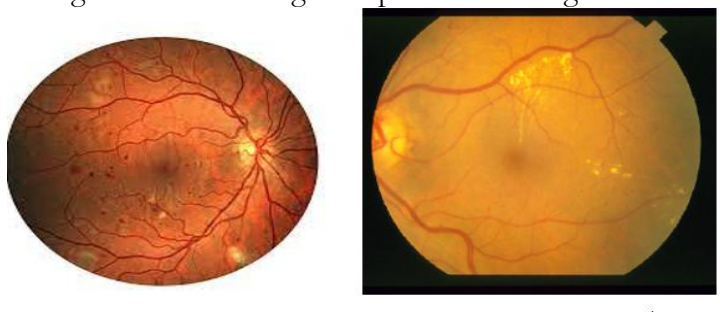
Dataset Description:

The STARE (Structured Analysis of the Retina) dataset is widely used for retinal image analysis, blood vessel segmentation, and disease detection systems. Hoover and Goldbaum captured the images at the University of California, San Diego. Each image is a high-resolution color fundus photo with a field of view of nearly 35 degrees. Each image is stored in Portable Pixmap Format (PPM), with a resolution of 700×605 pixels. Two observers (Observer A and Observer B) added their vessel annotations to the same images. Aside from vessel segmentation masks, the database contains images of healthy eyes and patients suffering from retinal conditions such as diabetic retinopathy, choroidal neovascularization, and central retinal vein occlusion. STARE is an important tool for educating and developing computer-aided eye care tools due to its extensive annotations and wide range of retinal conditions.



Data De-noising:

Data denoising is a critical step in reducing the number of photos in the input set that are irrelevant and cannot be upgraded. The input dataset is thoroughly visualized one by one, and the irrelevant images are sorted using the comparison technique. A network filter is applied to the dataset to measure the correlation between different images. Images with low correlation are then removed from the input dataset to improve classification performance. A sample of a noised image and a clear image is represented in Figure 2.

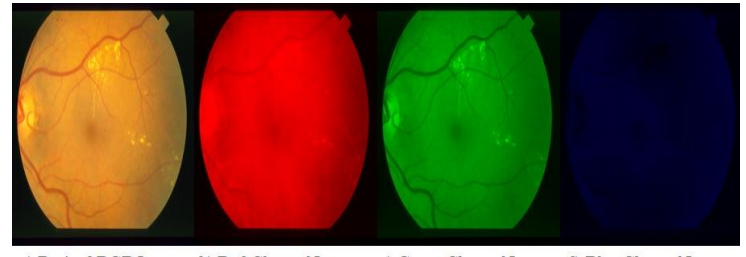


a) Noisy Image

Figure 2. Noise vs Denoised RFI [12].

Image Enhancement using CLAHE:

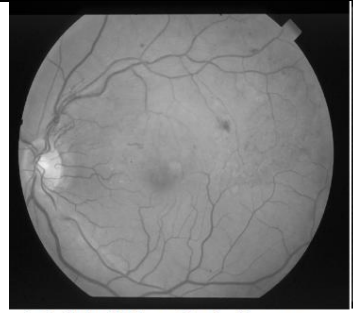
CLAHE executes Contrast-Limited Adaptive Histogram Equalization [34] on the image following all noise removal from the input image. CLAHE uses adjustable regions to examine the real brightness conditions that exist throughout an RGB color space image. Local color correction operates as a part of the proposed retinal fundus image procedure. The proposed system handles RFIs through sub-block segmentation before adding histograms across individual regions, unlike other approaches that work with channel-wide distributions. Smoothing is applied. The initial process inside CLAHE divides image channels into R, G, and B frames for separation purposes. Figure 3 presents an example image along with the separate images captured from the red, green, and blue color channels. Blood vessels are more clearly visible in the green channel because it has a lower noise level compared to the other channels.



a) Resized RGB Image b) Red Channel Image c) Green Channel Image d) Blue Channel Image Figure 3. RGB channels of RFI [34].

The Green Channel image received the CLAHE application first to enhance contrast levels. When you add the noise pattern (salt and pepper noise) to the original image noise it produces better filtering performance since natural noise cannot be deleted completely. Two successive filters including a median filter followed by a morphology filter eliminated the combined noise from the images. Utilizing two successive filters enabled the maximum possible attainment of noise filtering performance. The evaluation process continued after converting the Green Channel image into grayscale format.







a) Original Gray Scale Image

b) Improved Gray Scale Image

Figure 4. RFI enhancement using Green Channel.

Proposed Approach for Feature Extraction and Selection:

The proposed technique applied three sequential procedures. A CLAHE enhancement procedure operated on three channels to enhance the image during the first processing step. After enhancement, features were derived from multiple machine learning systems for three advanced models, which enabled the assembly of a superior feature collection. The selection of redundant features was performed using probability density analysis together with Euclidean distance measurements. BoDF operated to select the best features in the final step. The model architecture appears in Figure 5.

Model-A: AlexNet:

AlexNet [35] is the first Convolutional Neural Network (CNN) used to extract features from processed and improved images. AlexNet contains five convolutional-layer architectures with maximum pooling at three layers to reduce image size at each level. Enhanced images from CLAHE were fed into AlexNet's input layer, the input was rescaled to 227 x 227 x 3. Following convolution layers 1, 2, and 5, a 3 x 3 max pooling kernel with strides of 26 x 26 x 96, 12 x 12 x 256, and 5 x 5 x 256 is utilized. To concatenate all the gathered characteristics, the fully connected layers (FC) 3 and 7 were used. The output was a matrix, with rows representing features for each image and columns representing the deep feature attributes of the respective image. The output dimensions of the AlexNet architecture were 1186 x 4096.

Model-B: GoogLeNet:

In the proposed methodology, the second pre-trained model used was GoogLeNet [36], which had a 22-layer architecture. The images with dimensions 224 x 224 x 3 fed to the network which performs the feature extraction and with an output size of 1186 x 1000.

Model-C: ResNet-50:

ResNet-50 [37] contains 50-layer residual networks. This deep CNN also includes convolutional layers such as AlexNet and GoogLeNet. The classification layers of the ResNet model are not used because they are for 1000 classes, which can lead to misclassification. As a result, the model is trained up to the fully connected layer to extract features.

The features from all three trained networks were gathered and catenated to generate a composite feature vector (CFV) with the dimensions $1186 \times 3 \times 1000$. A subset of 1,000 attributes from AlexNet was selected to maintain a comparable set of matrices. Consequently, the total number of features amounted to 3,558,000. It takes a long time to test all these features with a classifier. As a result, the less relevant features were discarded, and only the high-quality features were selected in the subsequent stage.

Mutual Information: Redundant Feature Elimination:

Mutual information (MI) gives a number that quantifies the relationship between two random variables sampled at the same time. MI was used to choose features that had substantially the same association. This method makes use of the marginal and joint distributions of the variables X and Y. Let X represent the input photographs and Y represent



the relevant feature. P(X) and P(Y) reflect the random value's marginal distributions, while P (X, Y) indicates the joint distribution. The MI drives the following equation using these random values:

$$M.I(X,Y) = \sum_{x \in X} \sum_{y \in Y} P(X,Y) \log \frac{P(X,Y)}{P(X).P(Y)}$$

After applying feature elimination using the formula $CFV = F \times class$, the total number of features was reduced from 3558×1000 to 2900×1000 using the proposed methodology.

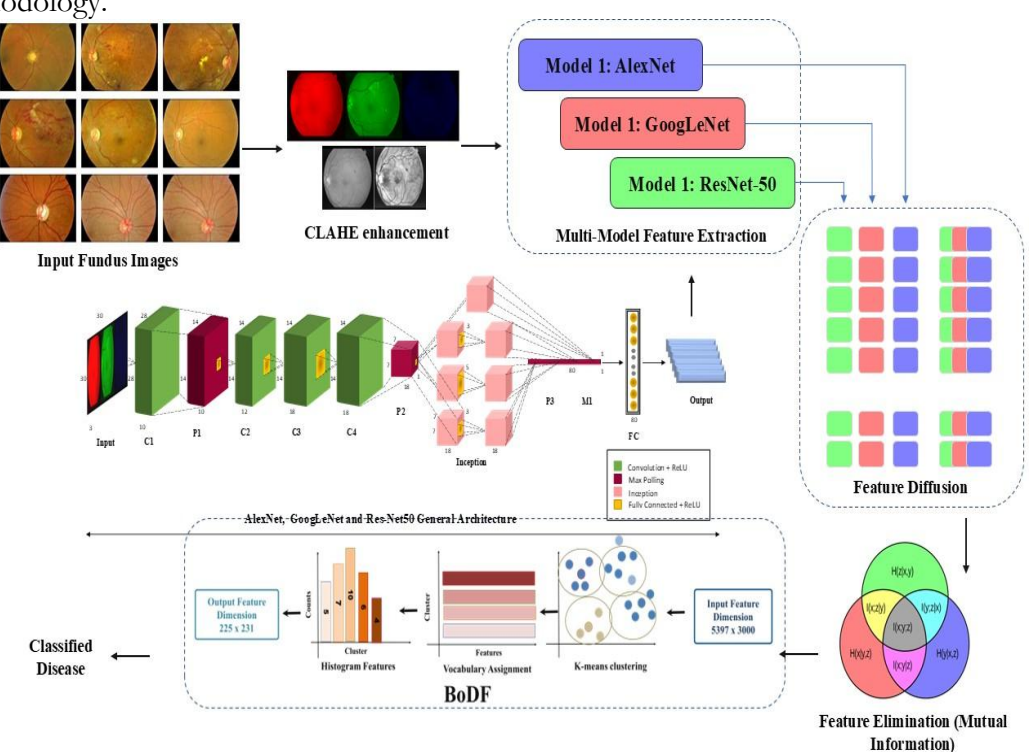


Figure 5. Proposed Scheme for Classifying Ocular Diseases BoDF: High-Quality Feature Selection:

Following the removal of redundant features, the quality features were chosen using the Bag of Deep Features (BoDF) [38]. BoDF serves as a mechanism for displaying only the most relevant features. Ultimately, this strategy helps reduce the computational cost of the model. This approach is commonly used in signal processing to compensate for anomalies. BoDF is a two-step technique that begins by grouping related features using the K-NN classifier [39]. Using K-NN at various "k" values, the centroids chosen are used as a vocabulary of the input set. Using the Euclidean distance formula, only those features from the vocabulary

$$ED(X_i, Y_j)_{wij} = \sqrt{\sum_{i=1}^{N} (X_i - C)^2 + \sum_{j=1}^{N} (Y_j - C)^2}$$

Following the selection of k with the lowest squared error, all the neighboring features were assigned a weight. $w_{ij} = \sum_{ij}^{N} [(x_i, y_j)] \triangleq \frac{1}{k}$, and the remainder will be 0. Where k= 1,2,3, N and N is the total number of features x and y are the rows and columns from the features where rows represent the features and y represents the attributes. From this equation, the centroid C is calculated.

For variables Xi and Yj, the asymptotic and asymptotic equation becomes:

that are closest to the centroids were chosen.



$$[S_{(X,Y)}]^2 = \sum_{i,j=1}^{N} (w_{ij})$$

and,

$$T_{Ni} = N^{\frac{-2}{ED}} \sum_{i=1}^{N} (w_{ij}) (i^{1+\frac{2}{ED}} - (1-i)^{1+\frac{2}{ED}})$$

$$T_{Nj} = N^{\frac{-2}{ED}} \sum_{j=1}^{N} (w_{ij}) (j^{1+\frac{2}{ED}} - (1-j)^{1+\frac{2}{ED}})$$

The second stage of the BoDF concerns the frequency of occurrence; during this stage, the system will automatically select the characteristic that occurs in a specific cluster. Using this strategy, the identical feature is considered only once, which is the cluster's centroid. The remaining functionalities were later removed. This is a straightforward and widespread method of picking quality attributes. To validate the quality of the features, the mean squared error of the model is determined for various k values. After passing through the BoDF mechanism, the feature values were further reduced to 250 × 1000, compared to the 2900 × 1000 output obtained from the RFE stage.

Selecting K Clusters:

To integrate similar features in BoDF, we employed the K-Nearest Neighbor (K-NN) Clustering algorithm. The choice of k is an iterative process that will take a long time. To better discover the value of k for all the classifiers, we calculated the mean squared error for each value of k.

	Algorithm 1: Detecting Ocular Disease using BoDF					
	Input: Digital Retinal Fundus Images from STARE dataset.					
	Output: Classification of Ocular Disease					
1	Step1: Data Preprocessing					
	Denoising: Apply Gaussian Filter to remove noise.					
	$I_{denoised\ (x,y)} = \frac{1}{2\pi\sigma^2} \sum_{i=-k}^{k} \sum_{i=-k}^{k} I_{(x-i,y-j)} \cdot \exp(-\frac{i^2 + j^2}{2\sigma^2})$					
	Enhancement using CLAHE: For each RGB channel apply CLAHE to					
	enhance contrast					
	$I_{enhanced\ (x,y)} = CLAHE(I_{denoised\ (x,y)})$					
2	Step2 Feature Extraction: using deep CNN models to extract features					
	AlexNet					
	$F_{alex} = CNN_{alex}(I_{enhanced})$					
	GoogleNet					
	$F_{google} = CNN_{google}(I_{enhanced})$					
	ResNet-50					
	$F_{res} = CNN_{res}(I_{enhanced})$					
3	Step 3 Feature Selection: merge the features to create a composite feature					
	vector.					
	$F_{composite} = [F_{alex}; F_{google}; F_{res}]$					
4	Apply BoDF and select high-quality features using M.I.					
	$F_{BODF} = BODF(F_{composite})$					
5	Eliminates similar features using MI					
	$F_{selected} = MI(F_{BODF})$					



6	Step-	Step4 Classification: Use classifiers to identify ocular disease at an early stage				
7		Support Vector Machine				
		$Class_{SVM} = SVM (F_{selected})$				
8		Decision Tree				
		$Class_{DT} = DT (F_{selected})$				
9	Step5 Evaluation: Compare the proposed model with current state-of-the-art					
	mod	els				
10		TP + TN				
		$Accuracy = {TP + TN + FP + FN}$				
11	end					

Classification:

In this study, transfer learning methodology was adopted, utilizing the CNN model only up to the fully connected (FC) layer. This is because the pre-trained model's classification layer is designed to handle up to 1000 classes. To prevent misclassification, binary or low-level kernel-based classifiers were employed instead. To classify disease, the two most generally accessible classifiers, Support Vector Machine and Decision Tree were utilized.

Support Vector Machine:

The Support Vector Machine Classifier distributes classes into two major classes of disease. Proposed model feature values with labels are fed to the SVM classifier to accurately predict the targeted values.

Decision Tree:

A Decision tree (DT) is a second classification classifier. This approach also allows for the diagnosis of many eye diseases. This categorization, unlike SVM, is an iterative procedure. This will take some time, but the accuracy gained is good when compared to other categorization models available.

Experimental Results:

This section presented the results produced through the proposed methodology. The retinal fundus images were enhanced in the first step of the model using three different colors from the R, G, and B scales. The model established distinct strategies for each of the three states. The enhanced photos were exhibited in the right column of Figure 6, while the original grayscale images were shown in the left column. Similarly, before extracting features from the supplied collection, all 1186 images in the dataset were enhanced.

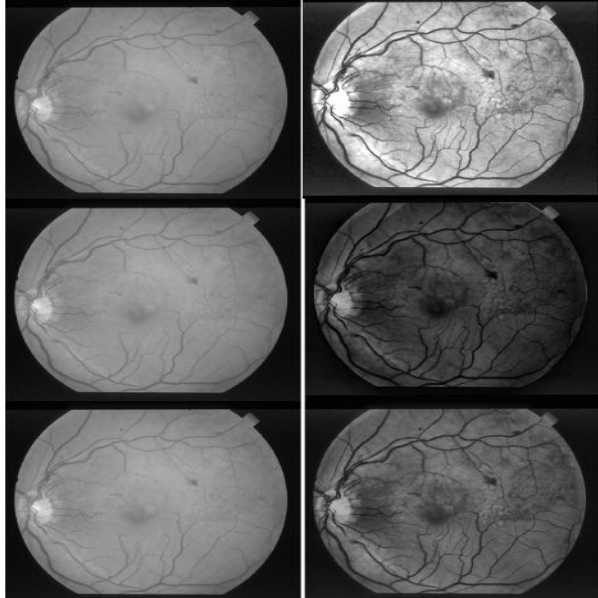


Figure 6. Retinal Fundus Image Enhancement using 3-level CLAHE process.



Support Vector Machine:

After extracting feature values and removing redundant features, the model was classified using SVM and DT one by one. The performance of the proposed model employing the SVM classifier is displayed in Table 1. The table shows that individual accuracy is achieved along with a satisfactory F1-score; however, testing for the disease will require additional training time. Similarly, the combined feature values indicate 91% accuracy but will eventually raise the train duration. To reduce this time, BoDF is employed, as shown in the table1, and the train time is reduced to 3.4 seconds with an overall classification accuracy of 94.8 % after applying BoDF on combined feature values.

Table 1. Mode	l Classification	Performance	using	SVM	Classifier

CNN Model	Feature vector	Accuracy	F1 Score	Sensitivity	Train time
CININ Model		$(^{0}/_{0})$			(Seconds)
AlexNet	1186 x 4096	84.5	0.87	0.75	128
GoogleNet	1186 x 1000	81.5	0.81	0.64	165
RestNet-50	1186 x 1000	89.3	0.77	0.81	181
Combined (Proposed)	3558 x 1000	91.6	0.89	8.99	3670
After RFE (Proposed)	2900 x 1000	93.1	0.86	0.93	2845
BODF Selected	250 x 340	94.8	0.91	0.93	3.4
(Proposed)					

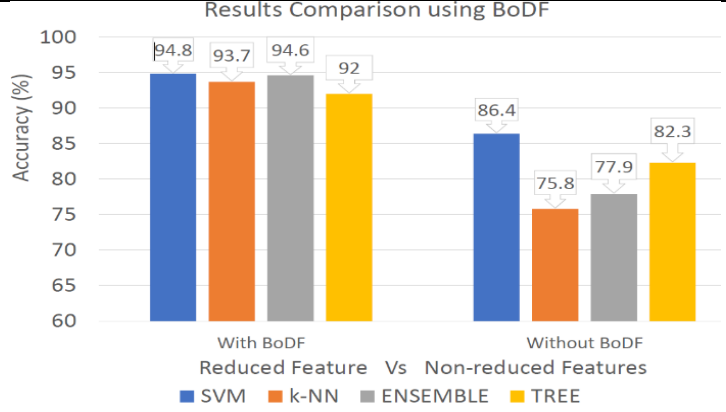


Figure 7. Result Comparison of Model with and without BoDF.

Figure 7 depicts a clear comparison of the model with and without BoDF. The suggested model indicates that ignoring low-quality features improves the model's performance and, as a result, reduces classification time. This method facilitates the rapid detection of all diseases and can also be effectively utilized for early-stage diagnosis.

Decision Tree:

The second model used for classification was DT. Table 2 shows the performance of the proposed model using the DT classifier. Individual accuracy can be achieved with a good F-1 score of 0.79, but evaluating the disease will require extra training time. Similarly, the combined feature values showed 91% correctness but eventually lengthened the training time. As indicated in Table 2, BoDF was used to reduce this time, and the training time was reduced to 12 seconds with an overall classification accuracy of 91.3% after applying BoDF on the combined feature values.

The Mean Squared Error (MSE) was calculated and displayed in Table 3 for all values of k ranging from 2 to 16. The table indicates that at k = 10 and k = 12, the normalized errors were observed with total feature counts of 354,578 and 247,764, respectively, from the combined feature values. In this work, k = 10 yielded superior classification performance.



Table 2. Model Classification Performance using DT Classifier.

CNN Model	Feature vector	Accuracy	F1 Score	Sensitivity	Train time
CININ Model		(%)			(Seconds)
AlexNet	1186 x 4096	80.2	0.84	0.77	218
GoogleNet	1186 x 1000	77.8	0.80	0.72	135
RestNet-50	1186 x 1000	83.1	0.87	0.88	225
Combined (Proposed)	3558 x 1000	90.9	0.91	0.81	3010
After RFE (Proposed)	2900 x 1000	89.6	0.75	0.89	2990
BODF Selected	250 x 340	91.3	0.88	0.77	12.6
(Proposed)					

Table 3. M Selection of k Cluster with total number of Features.

k	MSE (x106)	Cluster Features
2	84	265543
4	78	546783
6	57	33232
8	45	344744
10	10	45633
12	10	354578
14	11	247764
16	12	64773

Figures 8 and 9 demonstrate and depict the accuracy of the proposed model for different values of k for SVM and DT classifiers. The figures clearly show that the suggested model delivers good classification accuracies at k = 8, 10, and 12, which have low SME values.

SVM Classifier

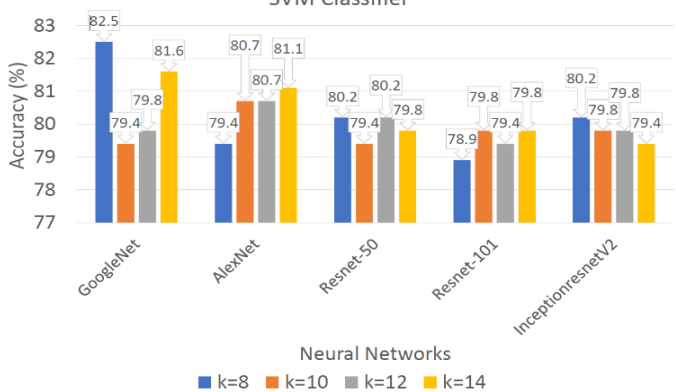


Figure 8. Accuracy of Model at different values of k using SVM Classifier.

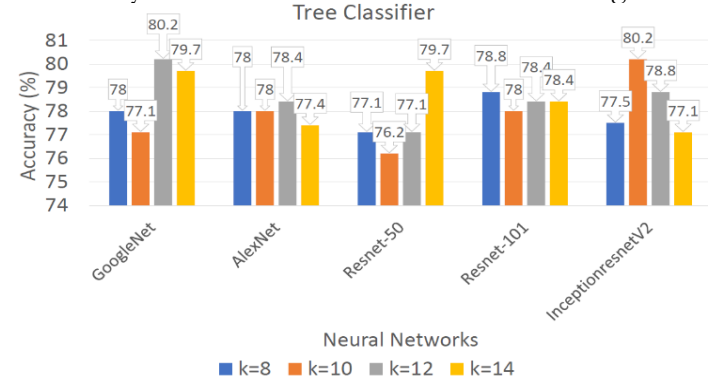


Figure 9. Accuracy of Model at different values of k using DT Classifier.

Discussion:

Multimodal CNN-BoDF has been shown where? to improve the accuracy of retinal disease classification. Figure 6 shows that by enhancing images with a 3-step CLAHE,

important features can be more easily identified and distinguished. All images were enhanced before being used for feature extraction, resulting in better model performance. The primary benefit of this method is that multiple CNN models (AlexNet, GoogleNet, and ResNet-50) are used to select and reduce features for each model. The combined feature vector improved accuracy (91.6% for SVM and 90.9% for DT), but it required significantly more training time.

Applying BoDF reduced the number of features, sped up training time, and improved classifier performance. BoDF reduced training time from 3,670 seconds to 3.4 seconds, while the SVM classifier increased accuracy from 91.6% to 94.8%. Similarly, using the decision tree classifier reduced training time from 3,010 seconds to 12.6 seconds, while improving model accuracy from 90.0% to 91.3%.

This suggests that, in areas with limited medical resources, avoiding unnecessary and ineffective features improves both the speed and accuracy of classification. The findings are shown in Table 3 and Figures 8 and 9. The mean square error (MSE) was lowest when k was 10 or 12, indicating that this value is the best fit for the number of clusters. SVM and DT demonstrated the highest accuracy, indicating that the clustering technique performed well.

This demonstrates that most existing models must sacrifice accuracy to achieve rapid detection, whereas the proposed method does not. A robust and efficient method for detecting ocular diseases can be achieved by selecting important features using improved image processing, multi-model CNNs, and BoDF. This model can help clinicians make decisions because of its accuracy, speed, and ability to detect diseases early.

Comparison with Recent Trends:

According to the comparison table, the suggested model outperforms previous studies in classification accuracy. It can be seen that the SVM classifier achieves higher classification accuracy when compared to eye-related disease detection using the SVM classifier shown in Table 4. This paper's BoDF model recognizes emotions without image deconstruction.

In comparison to several previously developed methods for detecting ocular diseases, the Multi-Model-CNN BoDF is more accurate and is capable of being used for early detection. Several previous studies used CNNs, SVMs, and LSTMs to study eye diseases such as glaucoma, diabetic retinopathy (DR), dry eye disease (DED), and age-related macular degeneration (AMD). Even though the models VGG-16 for DED on CNN and Decomposition CNN for glaucoma were accurate, with scores of 83.46% and 94%, respectively, they cannot be used in the early stages of the disease. Similarly, these two models; MobileNet v3 and LESH-SVM, achieved good accuracies of 93.5% and 93.1% for glaucoma and DR, respectively, but were designed to diagnose conditions later in their progression rather than early on. DenseNet-201 stood out with 82.1% accuracy in DED and DR, and few models could be used at this early stage. Despite this, the actual results were significantly worse than what the proposed model predicted. The Classification Learner Tool (MCLT) for DR inspection detected it with an accuracy of 65.5% only at the early stage, demonstrating that increasing accuracy frequently means delaying detection. Alternatively, Multi-Model-CNN BoDF provides superior results of 94.8% for several diseases, including glaucoma, diabetic retinopathy, AMD, and DED, and is intended for early detection. As a result, individuals can benefit from early and precise eye disease tests that can be easily administered in clinics.

Table 4. Comparison of the Proposed Model with Recent Trends.

Model	Disease	Classifier	Accuracy (%)	Applicable Early Stage	for
CNN (VGG-16)	DED	CNN	83.46	No	
2-dimensional variational Mode	Glaucoma	SVM	89.45	No	
Decomposition CNN	Glaucoma	CNN	94	No	



Gradient Boosted	Glaucoma	SVM	8.8	No
Decision trees				
MobileNet v3	Glaucoma	CNN	93.5	No
Local Energy Base	DR	SVM	93.1	No
Shape Histogram				
(LESH)				
DenseNet 201	DED, DR	SVM	82.1	Yes
U-NET	Central Serous	SVM	76.3	No
	Chorioretinopathy			
LSTM	AMD	LSTM	89.4	No
RES-NET-50	Glaucoma	CNN	92.7	No
FCL EffienectNet-B3	AMD	CNN	84.7	No
Classification Learner	DR	SVM	65.5	Yes
Tool (MCLT)				
DL Methods	AMD	SVM	84.0	No
Multi-Model-CNN	Glaucoma, DT,	SVM	94.8	Yes
BoDF (Proposed)	AMD and DAD			

Conclusion:

Ocular pathology is the study of diseases that affect the eyes. The purpose of this test was to improve the quality of retinal fundus photographs so that medical experts could appropriately detect Retinal Diseases. It is quite challenging to categorize all associated diseases using a single strategy when employing machine learning technology. The input images were improved using CLAHE to get good performance after denoising. In this paper, a multimodal system for classifying all ocular diseases is introduced. To achieve a high-quality feature set, features from various CNN models were diffused together in this manner. The dimension of the combined feature vector is lowered by utilizing Mutual Information and BoDF, which also aids in the selection of quality features. SVM and DT were then used to classify quality features. The proposed methodology is quite effective at detecting various ocular diseases. The results obtained when compared to comparable work reveal that the suggested model is quite effective as a state-of-the-art model.

Contributions:

With the onset of the fourth industrial revolution, more machine learning technologies are being investigated for the autonomous detection of ocular illnesses. To distinguish between these disorders, numerous machine learning models were presented. An efficient multi-model machine learning approach was put out in this paper to identify various ocular disorders. The proposed model was designed with the goal of offering superior classification performance with less computational overhead and quick processing.

The main contribution of this work is to design a generic model that can be able to classify three major ocular diseases, which is only possible by our proposed transfer learning and multi-model feature diffusion method. This contribution will lead researchers and medical assistants to classify all eye-related diseases with only one generalized method with good classification performance and in short processing time.

References:

- [1] A. R. Majeed, W. A. Awan, N. Ul Hassan, M. A. Asghar, and M. J. Khan, "Retinal Fundus Image Refinement with Contrast Limited Adaptive Histogram Equalization, Noise Filtration and Intensity Adjustment," *Proc. 2020 23rd IEEE Int. Multi-Topic Conf. INMIC 2020*, Nov. 2020, doi: 10.1109/INMIC50486.2020.9318104.
- [2] A. Shabbir *et al.*, "Detection of glaucoma using retinal fundus images: A comprehensive review," *Math. Biosci. Eng. 2021 32033*, vol. 18, no. 3, pp. 2033–2076, 2021, doi:

- 10.3934/MBE.2021106.
- [3] M. S. A. Ahsan Bin Tufail, Inam Ullah, Wali Ullah Khan, Muhammad Asif, Ijaz Ahmad, Yong-Kui Ma, Rahim Khan, Kalimullah, "Diagnosis of Diabetic Retinopathy through Retinal Fundus Images and 3D Convolutional Neural Networks with Limited Number of Samples," Wirel. Commun. Mob. Comput., 2021, doi: https://doi.org/10.1155/2021/6013448.
- [4] S. V. G.R. Sreekanth, R.S.Latha, R.C.Suganthe, S.Sivakumar, N.Swathi, K.Sonasri, "Automated Detection and Classification of Diabetic Retinopathy and Diabetic Macular Edema in Retinal Fundus Images Using Deep Learning Approach," NVEO Nat. Volatiles Essent. Oils, vol. 8, no. 5, 2021, [Online]. Available: https://www.nveo.org/index.php/journal/article/view/325
- [5] Y. Han *et al.*, "Application of an anomaly detection model to screen for ocular diseases using color retinal fundus images: Design and evaluation study," *J. Med. Internet Res.*, vol. 23, no. 7, p. e27822, Jul. 2021, doi: 10.2196/27822.
- [6] J. Nayak, P. S. Bhat, R. Acharya U, C. M. Lim, and M. Kagathi, "Automated identification of diabetic retinopathy stages using digital fundus images," *J. Med. Syst.*, vol. 32, no. 2, pp. 107–115, Apr. 2008, doi: 10.1007/S10916-007-9113-9/METRICS.
- [7] Early Treatment Diabetic Retinopathy Study Research Group,
 "PHOTOCOAGULATION FOR DIABETIC MACULAR EDEMA: EARLY
 TREATMENT DIABETIC RETINOPATHY STUDY REPORT NO. 4," Int.
 Ophthalmol. Clin., vol. 27, no. 4, pp. 265–272, 1987, [Online]. Available:
 https://journals.lww.com/internatophthalmology/citation/1987/02740/photocoagulation_for_diabetic_macular_edema_
 early.6.aspx
- [8] F. L. Ferris, "How Effective Are Treatments for Diabetic Retinopathy?," *JAMA*, vol. 269, no. 10, pp. 1290–1291, Mar. 1993, doi: 10.1001/JAMA.1993.03500100088034.
- [9] G. T. R Williams, S Nussey, R Humphry, "Assessment of non-mydriatic fundus photography in detection of diabetic retinopathy.," *Br Med J (Clin Res Ed)*, vol. 293, 1986, doi: https://doi.org/10.1136/bmj.293.6555.1140.
- [10] E. R. Higgs, B. A. Harney, A. Kelleher, and J. P. D. Reckless, "Detection of Diabetic Retinopathy in the Community Using a Non-mydriatic Camera," *Diabet. Med.*, vol. 8, no. 6, pp. 551–555, Jul. 1991, doi: 10.1111/J.1464-5491.1991.TB01650.X;WGROUP:STRING:PUBLICATION.
- [11] 7th edition Millodot: Dictionary of Optometry and Visual Science, "ocular pathology," Free Dict., 2009, [Online]. Available: https://medicaldictionary.thefreedictionary.com/ocular+pathology
- [12] E. B. R. and G. R. N. M. C. V. Stella Mary, "Retinal Fundus Image Analysis for Diagnosis of Glaucoma: A Comprehensive Survey," *IEEE Access*, vol. 4, pp. 4327–4354, 2016, [Online]. Available: https://ieeexplore.ieee.org/document/7536180
- [13] N. H. Butt, M. H. Ayub, and M. H. Ali, "Challenges in the management of glaucoma in developing countries," *Taiwan J. Ophthalmol.*, vol. 6, no. 3, pp. 119–122, 2016, [Online]. Available: https://www.sciencedirect.com/science/article/pii/S2211505616000090?via%3Dihub
- [14] J. M. & K. W. Rubina Sarki, Khandakar Ahmed, Hua Wang, Yanchun Zhang, "Image Preprocessing in Classification and Identification of Diabetic Eye Diseases," *Data Sci. Eng.*, vol. 6, pp. 455–47, 2021, [Online]. Available: https://link.springer.com/article/10.1007/s41019-021-00167-z
- [15] D. R. Parashar and D. K. Agarwal, "SVM based Supervised Machine Learning Framework for Glaucoma Classification using Retinal Fundus Images," *Proc. 2021 IEEE 10th Int. Conf. Commun. Syst. Netw. Technol. CSNT 2021*, pp. 660–663, 2021, doi: 10.1109/CSNT51715.2021.9509708.
- [16] T. N. Guangzhou An, Kazuko Omodaka, Kazuki Hashimoto, Satoru Tsuda, Yukihiro



- Shiga, Naoko Takada, Tsutomu Kikawa, Hideo Yokota, Masahiro Akiba, "Glaucoma Diagnosis with Machine Learning Based on Optical Coherence Tomography and Color Fundus Images," *J. Healthe. Eng.*, 2019, [Online]. Available: https://onlinelibrary.wiley.com/doi/10.1155/2019/4061313
- [17] G. An et al., "Comparison of Machine-Learning Classification Models for Glaucoma Management," J. Healthc. Eng., vol. 2018, Jun. 2018, doi: 10.1155/2018/6874765.
- [18] I. T. N. and R. K. M. T. Islam, S. T. Mashfu, A. Faisal, S. C. Siam, "Deep Learning-Based Glaucoma Detection With Cropped Optic Cup and Disc and Blood Vessel Segmentation," *IEEE Access*, vol. 10, pp. 2828–2841, 2022, [Online]. Available: https://ieeexplore.ieee.org/document/9664528
- [19] M. Chetoui, M. A. Akhloufi, and M. Kardouchi, "Diabetic Retinopathy Detection Using Machine Learning and Texture Features," *Can. Conf. Electr. Comput. Eng.*, vol. 2018-May, Aug. 2018, doi: 10.1109/CCECE.2018.8447809.
- [20] P. M. Nergis C. Khan, Chandrashan Perera, Eliot R. Dow, Karen M. Chen, Vinit B. Mahajan, "Predicting Systemic Health Features from Retinal Fundus Images Using Transfer-Learning-Based Artificial Intelligence Models," *Diagnostics*, vol. 12, no. 7, p. 1714, 2022, doi: https://doi.org/10.3390/diagnostics12071714.
- [21] Tae Keun Yoo; Bo Yi Kim; Hyun Kyo Jeong; Hong Kyu Kim; Donghyun Yang; Ik Hee Ryu, "Simple Code Implementation for Deep Learning–Based Segmentation to Evaluate Central Serous Chorioretinopathy in Fundus Photography," *Transl. Vis. Sci. Technol.*, vol. 11, no. 22, 2022, [Online]. Available: https://tvst.arvojournals.org/article.aspx?articleid=2778499
- [22] J. M. Arun Das, Paul Rad, Kim-Kwang Raymond Choo, Babak Nouhi, Jonathan Lish, "Distributed machine learning cloud teleophthalmology IoT for predicting AMD disease progression," *Futur. Gener. Comput. Syst.*, vol. 93, pp. 486–498, 2019, [Online]. Available: https://www.sciencedirect.com/science/article/abs/pii/S0167739X18317941?via%3Dih ub
- [23] M. K. Sidong Liu, Stuart L. Graham FRANZCO, Angela Schulz and B. Zangerl, "A Deep Learning-Based Algorithm Identifies Glaucomatous Discs Using Monoscopic Fundus Photographs," *Ophthalmol. Glaucoma*, vol. 1, no. 1, pp. 15–22, 2018, [Online]. Available: https://www.sciencedirect.com/science/article/abs/pii/S2589419618300127?via%3Dih ub
- [24] X. Luo, J. Li, M. Chen, X. Yang, and X. Li, "Ophthalmic Disease Detection via Deep Learning with a Novel Mixture Loss Function," *IEEE J. Biomed. Heal. Informatics*, vol. 25, no. 9, pp. 3332–3339, Sep. 2021, doi: 10.1109/JBHI.2021.3083605.
- [25] A. Al-Zebari and A. Sengur, "Performance Comparison of Machine Learning Techniques on Diabetes Disease Detection," 1st Int. Informatics Softw. Eng. Conf. Innov. Technol. Digit. Transform. IISEC 2019 Proc., Nov. 2019, doi: 10.1109/UBMYK48245.2019.8965542.
- [26] "Erratum: Promising Artificial Intelligence—Machine Learning—Deep Learning Algorithms in Ophthalmology: Erratum (Asia-Pacific Journal of Ophthalmology (2019) 8(3) (264–272), (S2162098923005066), (10.22608/APO.2018479))," *Asia-Pacific J. Ophthalmol.*, vol. 8, no. 5, p. 417, Sep. 2019, doi: 10.1097/01.APO.0000586388.81551.D0.
- [27] Z. W. & H. Z. Feng Li, Yuguang Wang, Tianyi Xu, Lin Dong, Lei Yan, Minshan Jiang, Xuedian Zhang, Hong Jiang, "Deep learning-based automated detection for diabetic retinopathy and diabetic macular oedema in retinal fundus photographs," *Eye*, vol. 36, pp. 1433–1441, 2022, [Online]. Available: https://www.nature.com/articles/s41433-021-01552-8
- [28] L. W. & W. H. Li Lu, Enliang Zhou, Wangshu Yu, Bin Chen, Peifang Ren, Qianyi Lu, Dian Qin, Lixian Lu, Qin He, Xuyuan Tang, Miaomiao Zhu, "Development of deep learning-based detecting systems for pathologic myopia using retinal fundus images," *Commun. Biol.*, vol. 4, no. 1225, 2021, [Online]. Available:



- https://www.nature.com/articles/s42003-021-02758-y
- [29] M. A. Anwer, G. A. Qattan, and A. M. Ali, "Ocular Disease Classification Using Different Kinds of Machine Learning Algorithms," *Zanco J. Pure Appl. Sci.*, vol. 36, no. 2, pp. 25–34, Apr. 2024, doi: 10.21271/ZJPAS.36.2.3.
- [30] M. D. Shumoos Al-Fahdawi, Alaa S. Al-Waisy, Diyar Qader Zeebaree, Rami Qahwaji, Hayder Natiq, Mazin Abed Mohammed, Jan Nedoma, Radek Martinek, "Fundus-DeepNet: Multi-label deep learning classification system for enhanced detection of multiple ocular diseases through data fusion of fundus images," *Inf. Fusion*, vol. 102, p. 102059, 2024, [Online]. Available: https://www.sciencedirect.com/science/article/pii/S1566253523003755?via%3Dihub
- [31] G. R. Asadi Srinivasulu, Clement Varaprasad Karu, G Sreenivasulu, "Automatic Detection and Classification of Eye Diseases from Retinal Images Using Deep Learning: A Comprehensive Research on the ODIR Dataset," *Adv. Eng. Intell. Syst.*, vol. 3, no. 1, 2024, [Online]. Available: https://aeis.bilijipub.com/article_193336_5671c20ca75ae01a7050ebaacfc668e5.pdf
- [32] C. Y.-A. Laberiano Andrade-Arenas, "Advances in the diagnosis of ocular diseases: an innovative approach through an expert system," *Bull. Electr. Eng. Informatics*, vol. 13, no. 4, 2024, [Online]. Available: https://doi.org/10.11591/eei.v13i4.7971
- [33] I. R. Moaz Osama Omar, Muhammed Jabran Abad Ali, Soliman Elias Qabillie, Ahmed Ibrahim Haji, Mohammed Bilal Takriti Takriti, Ahmed Hesham Atif, "Beyond Vision: Potential Role of AI-enabled Ocular Scans in the Prediction of Aging and Systemic Disorders," *Siriraj Med. J.*, 2024, doi: https://doi.org/10.33192/smj.v76i2.266303.
- [34] Karel Zuiderveld, "Contrast Limited Adaptive Histogram Equalization," *Graph. Gems*, pp. 474–485, 1994, [Online]. Available: https://www.sciencedirect.com/science/article/abs/pii/B9780123361561500616?via%3 Dihub
- [35] J. Z. Zheng-Wu Yuan, "Feature extraction and image retrieval based on AlexNet," *Eighth Int. Conf. Digit. Image Process. (ICDIP 2016)*, vol. 10033, 2016, [Online]. Available: https://www.spiedigitallibrary.org/conference-proceedings-of-spie/10033/1/Feature-extraction-and-image-retrieval-based-on-AlexNet/10.1117/12.2243849.full
- [36] R. A. Pedro Ballester, "On the Performance of GoogLeNet and AlexNet Applied to Sketches," *Proc. AAAI Conf. Artif. Intell.*, vol. 30, no. 1, 2016, [Online]. Available: https://ojs.aaai.org/index.php/AAAI/article/view/10171
- [37] L. Wen, X. Li, and L. Gao, "A transfer convolutional neural network for fault diagnosis based on ResNet-50," *Neural Comput. Appl.*, vol. 32, no. 10, pp. 6111–6124, May 2020, doi: 10.1007/S00521-019-04097-W/METRICS.
- [38] S. S. M. Muhammad Adeel Asghar, Muhammad Jamil Khan, Fawad, Yasar Amin, Muhammad Rizwan, MuhibUr Rahman, Salman Badnava, "EEG-Based Multi-Modal Emotion Recognition using Bag of Deep Features: An Optimal Feature Selection Approach," *Sensors*, vol. 19, no. 23, p. 5218, 2019, doi: https://doi.org/10.3390/s19235218.
- [39] G. Guo, H. Wang, D. Bell, Y. Bi, and K. Greer, "KNN Model-Based Approach in Classification," *Lect. Notes Comput. Sci. (including Subser. Lect. Notes Artif. Intell. Lect. Notes Bioinformatics)*, vol. 2888, pp. 986–996, 2003, doi: 10.1007/978-3-540-39964-3_62.



Copyright © by authors and 50Sea. This work is licensed under Creative Commons Attribution 4.0 International License.